Advances in Science and Technology Research Journal

Advances in Science and Technology Research Journal, 2025, 19(10), 212–222
https://doi.org/10.12913/22998624/207916
ISSN 2299-8624, License CC-BY 4.0

Received: 2025.06.11
Accepted: 2025.08.15
Published: 2025.09.01

Modeling the impact of hydroprocessed ester and fatty acids – synthetic paraffinic kerosene fuel properties and engine performance on emission characteristics and particle size distribution

Paula Kurzawska-Pietrowicz[1*], Remigiusz Jasiński[1], Marta Maciejewska[1]

[1] Faculty of Civil and Transport Engineering, Poznan University of Technology, ul. Marii Skłodowskiej-Curie 5, 60-965 Poznan, Poland
* Corresponding author's e-mail: paula.kurzawska@put.poznan.pl

ABSTRACT

The physicochemical properties of fuels and engine performance parameters have a significant impact on emissions. This study focused on modeling the influence of fuel properties and engine parameters on CO_2, CO, NO_x, and PM emissions, with particular attention to particulate matter emission indices and particle size distribution parameters, such as geometric mean diameter and geometric standard deviation. The models were developed based on the experiments conducted on a miniature jet engine (GTM 400) fueled with HEFA-SPK blends in various proportions. Multi-linear regression with data standardization was used for model development. The models identified which parameters have the greatest impact on specific emission indices and how variations in input parameters affect emission outcomes. Eighteen fuel properties and engine performance parameters were included in the model development, and all eleven resulting models showed good agreement with the measured data and were validated using separate test points. This research bridges a gap in the literature by modeling the impact of HEFA-SPK fuel properties on pollutant emissions in miniature jet engines, with an added focus on particle size distribution parameters. By evaluating alternative fuels, such as HEFA-SPK and their effect on emission characteristics, this study contributes to advancing sustainability in aviation propulsion systems.

Keywords: emission modeling, PM modeling, miniature jet engine, HEFA, SAF.

INTRODUCTION

The aviation sector is responsible for 2.8% of CO_2 emission of the total anthropogenic emissions [1]. As electrification of the aviation sector is one of the most difficult from other sectors, the sustainable aviation fuels (SAFs) are one of the easiest ways to reduce greenhouse gas emissions. According to ReFuelEU Aviation, in 2050 SAFs should be used in at least 63% of aviation fuel [2]. As SAFs are a drop-in fuel and do not need any infrastructure or engine changes, the physicochemical parameters are similar to conventional aviation fuel. Requirements and production pathways which are certified are described in ASTM D7566. Currently there are 8 certified production pathways to produce alternative aviation fuel: Fischer-Tropsch synthetic paraffinic kerosene (FT-SPK) certified in 2009, hydroprocessed ester and fatty acids (HEFA-SPK) certified in 2011, hydroprocessed fermented sugars to synthetic isoparaffins (HFS-SIP), certified in 2014, Fischer-Tropsch synthetic paraffinic kerosene with aromatics (FT-SPK/A) certified in 2015, alcohol-to-jet synthetic paraffinic kerosene (ATJ-SPK) certified in 2016, catalytic-hydrothermolysis synthesized kerosene (CH-SK or CHJ) certified in 2020, hydroprocessed hydrocarbons, esters and fatty acids synthetic paraffinic kerosene (HHC-SPK or HC-HEFA-SPK) also certified in 2020 and the last one certified pathway Alcohol to Jet Synthetic Kerosene with Aromatics (ATJ-SKA)

certified in 2023 [3]. Most of the certified pathways allow blending pure SAF with Jet A-1 in proportion of 50:50 [3].

SAF fuels can significantly reduce GHG (greenhouse gases, GHG) emissions from aviation sector and also other harmful exhaust gases, like hydrocarbons, carbon monoxide or particulate matter (PM). According to many studies, the use of SAF in aircraft engines can reduce PM emission by even 95% comparing to Jet A-1 (result for pure FT-SPK) [4]. Many studies show that PM number and mass can be reduced by 50–70% compared to Jet A-1 depending on the used SAF, tested engine and blending limit [4, 5]. Durdina et al. [6] showed that the addition of HEFA-SPK can reduce the geometric mean diameter of particles and geometric standard deviation of particles. For exhaust gases, researches carried out by Timko et al. [7] showed that fueling engine with neat FT-SPK can reduce emission of CO by 20% and NOx by 10% compared to conventional fuel.

The most used sustainable aviation fuel is HEFA-SPK, which in 2023 was supplied at 96 airports [8]. HEFA-SPK fuel primary was produced from oily biomass, like camelina, jatropha or algae, but currently also from wastes and residues, such as used cooking oil, food processing wastes, municipal solid wastes, agricultural and foresty residues like wheat straw, corn stover, palm kenel. Also, more energy crops are used nowadays, like castor bean, poplar, willow and miscanthus [9–11].

This research focused on emission modeling of exhaust emissions including carbon monoxide, carbon dioxide and nitrogen oxides as well as parameters of PM emission and distribution, depending on the engine performance and fuel properties. Models were developed based on own engine tests on a miniature jet engine GTM 400, supplied by blends of HEFA-SPK fuel and Jet A-1. This allowed modeling emission from this specific engine depending on fuel blend properties and selected engine performance parameters.

MATERIALS AND METHODS

Test engine and fuels

The fuels examined in the study were mixtures containing HEFA-SPK fuel and Jet A-1 in different proportions: 10%HEFA, 20%HEFA, 30%HEFA, 40%HEFA, 50%HEFA and pure Jet A-1. For each of the fuel blends, physicochemical parameters were measured, such as: density, hydrogen and carbon content, surface tension, conductivity, kinematic viscosity, flash point and distillation temperature of 50% fuel.

The tests were carried out on GTM 400, a miniature turbine engine with maximum thrust of 400N. The engine consists of one stage radial compressor, annular combustion chamber and one stage axial turbine. Specific parameters of GTM 400 are presented in Table 1.

Apparatus and procedures

During the tests, an EEPS 3090 (Engine Exhaust Particulate Sizer™ spectrometer) analyzer was used for PM concentration measurement. EEPS 3090 measures the discrete range of particle diameter from 5.6 nm to 560 nm [12]. The technical parameters of an EEPS 3090 analyzer are presented in Table 2. The measuring probe was made of stainless steel and placed perpendicular to the engine outlet. EEPS 3090 measures particles number concentration and particle size distribution. To present particles mass concentration or volume-based particle size distribution, appropriate calculations assuming particle density have been conducted. The particles are treated as spheres with a uniform distribution of density based on a specific model. The density change curve, which was established through empirical findings for particles from a jet engine, was taken into account [13].

Also, the gaseous exhaust emissions were measured during the tests. For this purpose, a Semtech DS analyzer was used, which can measure the concentration of nitrogen oxides, carbon dioxide, carbon monoxide and hydrocarbons. The exhaust emissions from engine were directed to the analyzer through a cable with a temperature of 191 °C, which is essential for the accurate measurement of hydrocarbons in the flame ionization analyzer. After the measurement of hydrocarbons, the exhaust gases are cooled to the temperature of 4 °C which is required to properly measure the concentration of nitrogen oxides, carbon monoxide and carbon dioxide. The Semtech DS analyzer includes the following measurement modules: a flame ionization detector (FID), a non-dispersive ultraviolet (NDUV) analyzer, a non-dispersive infrared (NDIR) analyzer and an electrochemical analyzer [12, 14].

Table 1. Specific parameters of GTM 400

Parameter	Unit	Value
Thrust max.	N	400
Thrust min.	N	15
RPM max	rpm	85 000
RPM min	rpm	27 000
Compression ratio	-	3,3:1
Mass air flow rate	g/s	770
Exhaust gas temperature	°C	750
Fuel consumption	g/min	1200

Table 2. Technical parameters of EEPS 3090 [12]

Parameter	Value
Diameter range	5.6–560 nm
Number of measurement channels per decade	16
Resolution	10 Hz
Exhaust sample volume flow rate	0.6 m³/h
Compressed air volume flow rate	2.4 m³/h
Input sample temperature	10–52 °C

The tests were carried out for every selected fuel from 10% of maximum thrust to 100% of maximum thrust with step of every 10%. On every measurement point the engine worked for 20 seconds and the results are the average value of the 20 seconds measurements.

Modeling

The chosen modeling approach is multi-linear regression. The impact of the fuel properties and engine performance parameters can be described as followed:

$$Y = f(x_1, x_2, \ldots, x_k) + \varepsilon \tag{1}$$

where: Y – dependent variable explained by the model, $x_1, x_2, \ldots x_k$ – explanatory variables, ε – random component.

The multi-linear regression can be described as followed [16]:

$$Y = \beta_0 + \beta_1 x_1 + \beta_2 x_2 + \cdots + \beta_k x_k + \varepsilon \tag{2}$$

where: β_0 – constant term, $\beta_1, \beta_2, \ldots \beta_k$ – structural parameters of the model.

The modeling criteria for multi-linear regression are directed towards maximizing the R Square value while ensuring that each included parameter maintains a significance level below 5%, which is p-value ≤ 0.05. The chosen multi-linear regression is backward stepwise regression, which is achieved by incorporating statistical significance testing, in which dependent values are removed after each iteration. The modeling begins with all possible variables in the model and subsequently, variables with p-value higher than established are removed from the model. After removing non-significant variables the statistical significance is tested again, after every rejected variable. The process is continued after all selected variables are statistically significant [1, 15, 16].

All explanatory variables and dependent variables were standardized, to better compare the structural parameters and the influence of the input parameters on the dependent variable. After the predicted value calculation based on developed model, the final value of the dependent value should be re-standardized to find out the predicted value. The re-standardization can be calculated as follows:

$$X = Z\sigma + \mu \tag{3}$$

where: X – original value, Z – standardized value, σ – standard deviation of the original value, μ – mean value of the original data.

In this research, the physicochemical parameters of fuels blends and parameters measured during the engine tests on GTM-400 with all described HEFA-SPK blends were taken into model construction. During the study, 80% of the data was used to build the model and a randomly selected 20% was used to validate the model. Each model was considered in terms of the presented 18 parameters as explanatory variables presented in Table 3. For these parameters, VIF (Variance Inflation Factor) was calculated, which allows determining whether there is collinearity between the introduced explanatory variables. Final parameters with VIF below 5, were: total mass flow TMF, temperature at combustion chamber exit T3, fuel density ρ, fuel surface tension γ and flash point FP. After modeling process, when all of the coefficients had p-value < 0.05 and p-value for F-Snedecor test for the model was also below 0.05, the analysis of the normality of the distribution of residuals was performed using the Shapiro-Wilk test. If the Shapiro-Wilk test showed that there is no basis for

Table 3. All analyzed explanatory variables

Parameter	Symbol	Parameter	Symbol
Temperature at compressor diffuser [°C]	T_2	Fuel flow [ml/min]	FF
Temperature at combustion chamber exit [°C]	T_3	Kinematic viscosity [mm²/s]	v
Pressure at compressor diffuser [hPa]	P_2	Density [g/L]	ρ
Ambient temperature [°C]	AIRt	Flash point [°C]	FP
Turbine inlet temperature [°C]	TIT	Surface tension [mN/m]	γ
Temperature at the exhaust nozzle [°C]	EGT	Conductivity [pS/m]	σ
Total mass flow [kg/s]	TMF	Distillation temperature 50% [°C]	T50
Thrust [%]	F	Hydrogen [%]	H
Rotation speed [1/min]	RPM	Carbon [%]	C

rejecting the hypothesis of normality of the distribution of the data studied, the validation process were conducted [17, 18]. For validation there were used measurements points which were not taken in model development. That was 20% of all measured data which was randomly selected.

The final models were created for emission of CO_2, CO and NOx and PM parameters. For particulate matter, the models were made for particles intensity (E_{PNF}) [1/s], particulate matter emission rate (E_{PMF}) [g/h], the W_{PNF} [1/kg] which is a coefficient determining the number of particles produced from one kilogram of fuel used, W_{PMF} [mg/kg] which is a coefficient defining the mass of PM produced from one kilogram of fuel and also the models were made for parameters of particle distribution, such as diameter geometric mean and standard deviation. Particle distribution was similar in every measured point, and to model the distribution parameter, the Geometric mean diameter (GMD) and geometric standard deviation (GSD) has been calculated based on following formulas [19]:

$$GMD = exp\left[\frac{\sum nlnD_p}{N}\right] \tag{4}$$

$$GSD = exp\left[\frac{\sum n\left[lnD_p - lnGMD\right]^2}{N}\right]^{\frac{1}{2}} \tag{5}$$

where: n – concentration number of particular diameter, N – total concentration, D_p – particle diameter.

These formulas are accurate for particles number, and for geometric mean and geometric standard deviation of particulate matter mass, the n and N is changed by m and M, which are its equivalents.

RESULTS ANS DISCUSSION

Models of exhaust gases

Parameters of the NOx emission (E_{NOx}) model are shown in Table 4. The R-squared is equal to 0.983 and the standard error for model is 0.131. The F-statistic is 633.9 and the F significance is <0.05. Mean value for E_{NOx} is 0.00773 g/s and standard deviation is 0.00273. For Shapiro-Wilk test (0.977) the p-value was 0.463 so there is no basis for rejecting the hypothesis of normality of the residues distribution.

TMF has the greatest impact on NOx emission in this specific jet engine, in which increase of 1 standard deviation increases the E_{NOx} of 0.74 standard deviation. The second important parameter is flash point, in which increase of 1 standard deviation increases the E_{NOx} of 0.37 standard deviation, and also T3, in which increase of 1 standard deviation increases the NOx emission of 0.22 of standard deviation. The lowest coefficient has density, in which increase of 1 standard deviation decreases the NOx emission of 0.098 standard deviation.

The final model of standardized NOx emission is:

$$E_{NOx}\left[\frac{g}{s}\right] = 0.73598 \cdot TMF + \\ + 0.36618 \cdot FP - 0.09846 \cdot \rho + \\ + 0.22386 \cdot T_3 \pm 0.131 \tag{6}$$

For CO_2 emission (E_{CO2}), the regression model parameters are shown in Table 5. For this model the R-squared is equal to 0.995 and the standard error for model is 0.074. The F-statistic is 4342.07 and the F significance is < 0.05. Mean value for E_{CO2} is 6.159 g/s and standard deviation is 2.374. For Shapiro-Wilk test (0.845) the p-value is < 0.05, so the null hypothesis that

Table 4. Modeling results for NOx emission

Variable	Coefficient	Standard error	t Stat	p-value	VIF
TMF	0.73598	0.027	27.450	0.000	1.978
FP	0.36618	0.021	17.450	0.000	1.107
ρ	-0.09846	0.019	-5.144	0.000	1.102
T_3	0.22386	0.028	8.119	0.000	2.097

Table 5. Modeling results for CO_2 emission

Variable	Coefficient	Standard error	t Stat	p-value	VIF
TMF	0.89041	0.015	60.997	0.000	1.857
T_3	0.14965	0.015	10.264	0.000	1.857

the distribution of residuals is normal is rejected and there is evidence that the data tested are not normally distributed. This model can be used for CO_2 emission prediction, but it cannot be analyzed in terms of the impact of individual parameters on CO_2 emission.

The final model of standardized CO_2 emission is:

$$E_{CO2}\left[\frac{g}{s}\right] = 0.89041 \cdot TMF + \\ + 0.14965 \cdot T_3 \pm 0.074 \quad (7)$$

For CO emission (E_{CO}), the regression model parameters are shown in Table 6. For this model the R-squared is equal to 0.981 and the standard error for model is 0.143. The F-statistic is 777.42 and the F significance is < 0.05. Mean value for E_{CO} is 0.312 g/s and standard deviation is 0.112. For Shapiro-Wilk test (0.845) the p-value is < 0.05 so null the hypothesis that the distribution of residuals is normal is rejected and there is evidence that the data tested are not normally distributed. This model also can be used for CO emission prediction, but it cannot be analyzed in terms of the impact of individual parameters on CO emission.

The final model of standardized CO emission is:

$$E_{CO}\left[\frac{g}{s}\right] = 0.68035 \cdot TMF + \\ + 0.40757 \cdot T_3 + 0.07315 \cdot \gamma \pm 0.143 \quad (8)$$

Models of PM emissions indices

For particle intensity E_{PNF} [1/s] the model results are shown in Table 7. The R-squared is equal to 0.924 and the standard error for model is 0.265. The F-statistic is 133.76 and the F significance is < 0.05. Mean value for E_{PNF} is $8.1 \cdot 10^{13}$ particles/s and standard deviation is $2.7 \cdot 10^{13}$. For Shapiro-Wilk test (0.981) the p-value is 0.624 so there is no basis for rejecting the hypothesis of normality of the residues distribution.

T_3 has the greatest impact on E_{PNF}, an which increase of 1 standard deviation decreases the particle intensity of 1.23 standard deviation. The second parameter with the greatest absolute coefficient value is TMF, in which increase of 1 standard deviation increases E_{PNF} of 0.56 standard deviation. For flash point, the increase of 1 standard deviation cause an E_{PNF} decrease of 0.27 standard deviation and for density the increase of 1 standard deviation increases the particles intensity of 0.093 standard deviation.

The final model of standardized particles intensity [1/s] is:

$$E_{PNF}\left[\frac{1}{s}\right] = 0.56090 \cdot TMF - \\ -1.22645 \cdot T_3 - 0.27369 \cdot FP + \\ + 0.09266 \cdot \rho \pm 0.265 \quad (9)$$

For W_{PNF} [particles/kg of fuel] the model results are presented in Table 8. The R-squared for this model is 0.76, the standard error is 0.158, the F-statistic is 619.59 and the F significance is < 0.05. Mean value for W_{PNF} is $1.4 \cdot 10^{16}$ 1/kg and standard deviation is $6.2 \cdot 10^{15}$. For Shapiro-Wilk test (0.980) the p-value is 0.582 so there is no basis for rejecting the hypothesis of normality of the residues distribution.

T_3 has the greatest impact on W_{PNF}, an increase of 1 standard deviation de-creases the W_{PNF} of 0.65 standard deviation. Also increase of 1 standard deviation of TMF and FP decreases the W_{PNF} of appropriately 0.44 and 0.21 standard deviation.

Table 6. Modeling results for CO emission

Variable	Coefficient	Standard error	t Stat	p-value	VIF
TMF	0.68035	0.029	23.637	0.000	1.979
T_3	0.40757	0.029	13.981	0.000	1.925
γ	*0.07315*	0.022	3.259	0.002	1.066

Table 7. Modeling results for E_{PNF}

Variable	Coefficient	Standard error	t Stat	p-value	VIF
TMF	0.56090	0.054	10.332	0.000	1.978
T_3	-1.22645	0.056	-21.968	0.000	2.097
FP	-0.27369	0.042	-6.442	0.000	1.107
ρ	0.09266	0.039	2.391	0.021	1.023

The final model of standardized W_{PNF} [1/kg] is:

$$W_{PNF}\left[\frac{1}{kg}\right] = -0.43692 \cdot TMF - \\ -0.64699 \cdot T_3 - 0.20541 \cdot FP \pm 0.158 \quad (10)$$

For particle intensity E_{PMF} [g/h] the model results are shown in Table 9. The R-squared is equal to 0.64, the standard error is 0.594, the F-statistic is 41.04 and the F significance is < 0.05. Mean value for E_{PMF} is 1.179 g/h and standard deviation is 0.774. For Shapiro-Wilk test (0.956) the p-value is 0.07 so there is no basis for rejecting the hypothesis of normality of the residues distribution.

T_3 also has the greatest impact on E_{PMF}, an increase of 1 standard deviation decreases the E_{PMF} of 0.79 standard deviation. An increase of 1 standard deviation of surface tension decreases the E_{PMF} of 0.198 standard deviation.

The final model of standardized particulate matter emission rate [g/h] is:

$$E_{PMF}\left[\frac{g}{h}\right] = -0.79027 \cdot T_3 - \\ -0.19804 \cdot \gamma \pm 0.594 \quad (11)$$

For particle intensity W_{PMF} [mg/kg] the model results are shown in Table 10. The R-squared is equal to 0.842 and the standard error for model is 0.411. The F-statistic is 79.14 and the F significance is < 0.05. Mean value for W_{PMF} is 64.30 mg/kg and standard deviation is 43.56. For Shapiro-Wilk test (0.978) the p-value is 0.483 so there is no basis for rejecting the hypothesis of normality of the residues distribution.

T3 has the greatest impact on W_{PMF}, an increase of 1 standard deviation decreases the W_{PMF} of 0.71 standard deviation. Also, an increase of 1 standard deviation of FP and TMF decreases the W_{PMF} of appropriately 0.25 and 0.28 standard deviation.

The final model of standardized W_{PMF} [mg/kg] is:

$$W_{PMF}\left[\frac{mg}{kg}\right] = -0.28223 \cdot TMF - \\ -0.71454 \cdot T_3 - 0.24587 \cdot FP \pm 0.411 \quad (12)$$

Models of particle size distribution parameters

To describe particle size distribution for number and mass concentration, the diameter geometric mean and diameter standard deviation were calculated. The final model results for geometric mean diameter for number concentration (GMDn) are shown in Table 11. The R-squared is equal to 0.941 and the standard error for model is 0.251. The F-statistic is 238.11 and the F significance is < 0.05. Mean value for GMDn is 14.33 nm and standard deviation is 3.01. For Shapiro-Wilk test (0.986) the

Table 8. Modeling results for W_{PNF}

Variable	Coefficient	Standard error	t Stat	p-value	VIF
TMF	-0.43692	0.032	-13.566	0.000	1.962
T_3	-0.64699	0.033	-19.654	0.000	2.054
FP	-0.20541	0.025	-8.115	0.000	1.107

Table 9. Modeling results for E_{PMF}

Variable	Coefficient	Standard error	t Stat	p-value	VIF
T_3	-0.79027	0.087	-9.036	0.000	1.029
γ	-0.19804	0.092	-2.159	0.036	1.029

Table 10. Modeling results for W_{PMF}

Variable	Coefficient	Standard error	t Stat	p-value	VIF
TMF	-0.28223	0.084	-3.377	0.002	1.962
T_3	-0.71454	0.085	-8.364	0.000	2.054
FP	-0.24587	0.066	-3.743	0.001	1.106

p-value is 0.838 so there is no basis for rejecting the hypothesis of normality of the residue distribution.

Again T_3 has the greatest impact on GMDn, an increase of 1 standard deviation decreases the GMDn of 0.796 standard deviation. An increase of TMF and FP decreases the GMDn of appropriately 0.26 and 0.16 standard deviation.

The final model of standardized GMDn is:

$$GMDn\,[nm] = -0.25631 \cdot TMF - \\ - 0.79589 \cdot T_3 - 0.15736 \cdot FP \pm 0.251 \quad (13)$$

As far as the geometric standard deviation for GSDn is concerned, the model results are presented in Table 12. The parameters of this model are: R-squared equal to 0.951, the standard error is 0.238, the F statistic value is equal to 291.45 and F significance < 0.05. Mean value for GSDn is 1.411 and standard deviation is 0.065. For Shapiro-Wilk test (0.965) the p-value is 0.168 so there is no basis for rejecting the hypothesis of normality of the residues distribution.

T_3 has the greatest impact on GSDm, an increase of 1 standard deviation decreases the GSDn of 0.72 standard deviation, and an increase of 1 standard deviation of TMF and FP also decreases the GSDn of 0.39 and 0.14 standard deviation.

The final model of standardized GSDn is:

$$GSDn = -0.39232 \cdot TMF - \\ - 0.72348 \cdot T_3 - 0.13504 \cdot FP \pm 0.238 \quad (14)$$

For geometric mean diameter for particles mass concentration (GMDm), the model results are presented in Table 13. The parameters of this model are: R-squared equal to 0.635, standard error equal to 0.479, F statistic value is 26.12 and F significance <0.05. Mean value for GMDm is 23.542 and standard deviation is 2.765. For Shapiro-Wilk test (0.962) the p-value is 0.122 so there is no basis for rejecting the hypothesis of normality of the residues distribution. As for primary selected explanatory variables with low VIF value, for GMDm parameter none of the selected variables had p-value <0.05. Thus, for model development, other explanatory variables were taken into consideration, depending on the p-value of coefficients. As R squared and other statistic tests are at satisfactory level, the VIF for new selected variables is high, what suggest that the multicollinearity can be high and it is difficult to properly interpret the obtained results. Although the model works well just for GMDm prediction.

The final model of standardized GMDm is:

$$GMDm\,[nm] = -6.6787 \cdot T_2 + \\ + 7.0266 \cdot FF - 0.7052 \cdot T_3 \pm 0.479 \quad (15)$$

For geometric standard deviation for GSDm the model results are presented in Table 14. The parameters of this model are: R-squared equal to 0.884, standard error equal to 0.356, the F statistic value equal to 114.03 and F significance is <0.05.

Table 11. Modeling results for GMDn

Variable	Coefficient	Standard error	t Stat	p-value	VIF
TMF	-0.25631	0.051	-5.015	0.000	2.054
T_3	-0.79589	0.052	-15.235	0.000	1.962
FP	-0.15736	0.040	-3.917	0.000	1.107

Table 12. Modeling results for GSDn

Variable	Coefficient	Standard error	t Stat	p-value	VIF
TMF	-0.39232	0.048	-8.108	0.000	2.054
T_3	-0.72348	0.049	-14.629	0.000	1.962
FP	-0.13504	0.038	-3.551	0.001	1.107

Table 13. Modeling results for GMDm

Variable	Coefficient	Standard error	t Stat	p-value	VIF
T_2	-6.6787	0.840	-7.952	0.000	3.47
FF	7.0266	0.905	7.761	0.000	>10
T_3	-0.7052	0.130	-5.444	0.000	>10

Mean value for GSDm is 1.868 and standard deviation is 0.57. For Shapiro-Wilk test (0.954) the p-value is 0.059 so there is no basis for rejecting the hypothesis of normality of the residues distribution.

T_3 has the greatest impact on GSDm, an increase of 1 standard deviation in-creases the GSDm of 0.76 standard deviation. An increase of 1 standard deviation of TMF and surface tension increases the GSDn of 0.27 and 0.12 standard deviation.

The final model of standardized GSDm is:

$$GSDm = 0.27038 \cdot TMF + \\ + 0.75891 \cdot T_3 + 0.12455 \cdot \gamma \pm 0.356 \quad (16)$$

Model validation

Developed models based on measured point of GTM 400 for 6 fuel blends allow indicating important fuel and engine parameters that impact the emission parameters. Statistical parameters for developed models are presented in Table 15. As presented models were made for 80% of measurement points, 20% randomly selected measurement points were used for models validation. In order to compare the actual and predicted data, the graphs shown in Figures 1 and 2 are presented. Also specific validation parameters are shown in Table 15. Root mean square error (RMSE) is an average expected difference between predicted and actual value. Mean absolute error (MAE) shows the mean absolute error between the predicted and actual values and R^2 represents the proportion of the variance for a dependent variable that's explained by an independent variable.

For most presented models, the R^2 for validation is high and close to 1 and for E_{PMF}, W_{PMF}, GSDn and GMDm the fit is smaller. That can suggests that linear model used in this research is not suitable for this specific parameters, especially for emission indices of particulate matter mass. Modeling parameters suggesting a non-linear relationship between variables are, for example, the distribution of residuals, which in these specific cases is not randomly scattered around zero, but is arranged in specific patterns, which may suggest the non-linearity of the model [15]. All other parameters are well described by the models with very well fit between actual and predicted values.

CONCLUSIONS

To reduce the environmental impact of the aviation sector, it is crucial to develop new ecological technologies and improve existing ones. Sustainable aviation fuels (SAFs) represent a promising solution for reducing the emissions from aviation and remain an active area of research. New production pathways for alternative

Table 14. Modeling results for GSDm

Variable	Coefficient	Standard error	t Stat	p-value	VIF
TMF	0.27038	0.072	3.769	0.000	1.979
T_3	0.75891	0.073	10.444	0.000	1.925
γ	0.12455	0.056	2.226	0.031	1.066

Table 15. Parameters of developed emission models

Parameter	E_{NOx}	E_{CO2}	E_{CO}	E_{PNF}	W_{PNF}	E_{PMF}	W_{PMF}	GMDn	GSDn	GMDm	GSDm
Models based on 80% of data											
R^2	0.983	0.995	0.981	0.924	0.976	0.641	0.842	0.941	0.951	0.635	0.884
F significancy	<0.05	<0.05	<0.05	<0.05	<0.05	<0.05	<0.05	<0.05	<0.05	<0.05	<0.05
X variables no.	4	2	3	4	3	2	3	3	3	3	3
Validation for 20% of data											
R^2	0.94	0.97	0.90	0.93	0.91	0.63	0.56	0.84	0.30	0.47	0.81
RMSE	0.00	0.40	0.03	9.59e+12	1.73e+15	0.50	25.83	1.10	0.03	3.91	0.22

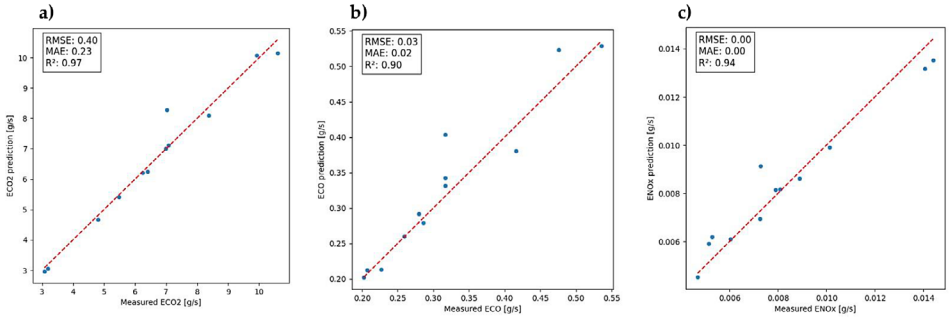

Figure 1. Graphs of measured and predicted emission parameters: a) E_{CO2}, b) E_{CO}, c) E_{NOx}

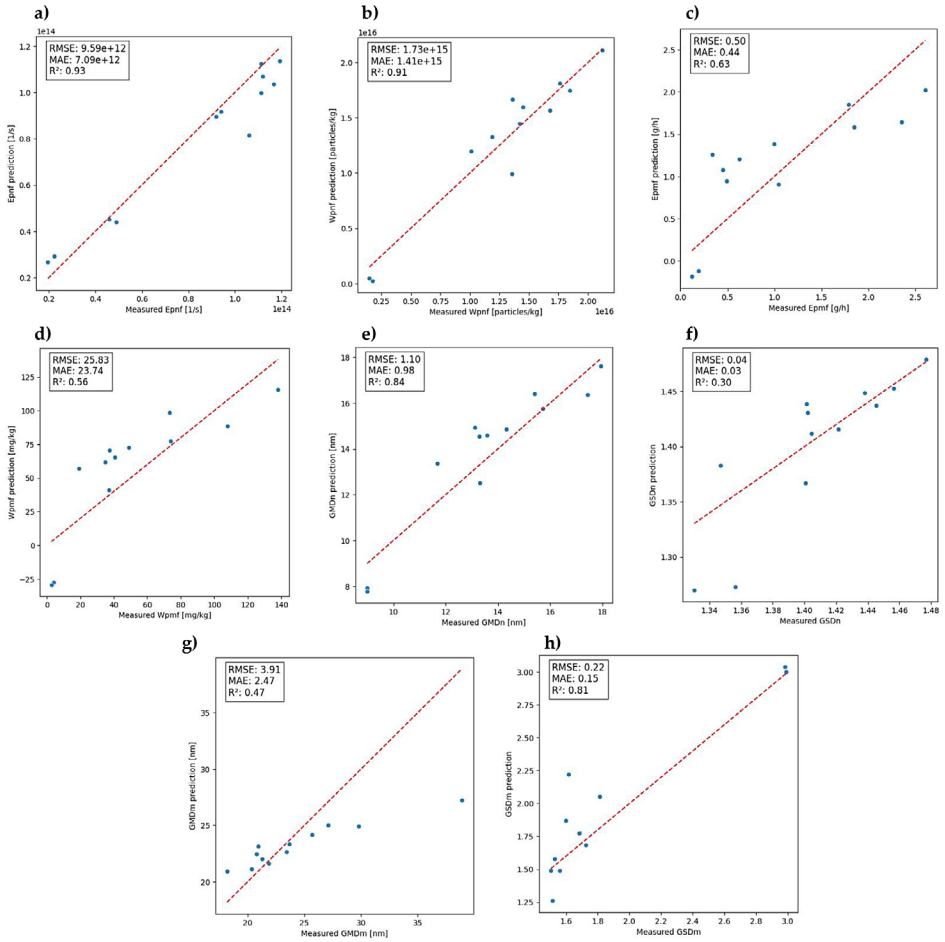

Figure 2. Graphs of measured and predicted emission parameters: a) E_{PNF}, b) W_{PNF}, c) E_{PMF}, d) W_{PMF}, e) GMDn, f) GSDn, g) GMDm and h) GSDm

aviation fuels are continuously being tested and approved under ASTM D7566. The tests involving the use of pure SAF in aircraft engines are ongoing, and research shows that 100% SAF can significantly reduce greenhouse gas and particulate matter emissions. Moreover, even blending SAF with conventional jet fuel yields impressive results in emission reduction compared to Jet A-1. The continued development and implementation of SAFs is essential for achieving long-term sustainability goals in the aviation industry.

Composition of SAF can change depending on used raw materials and production pathway and there is still a possibility to adjust the chemical composition of the fuel and its physicochemical properties so that emissions during its combustion in an aircraft engine are even lower. Emission modeling can find a parameters of fuel or engine performance, which influence the emission results the most and point a parameters which could be improved to reduce emission of particular pollutant. In this research an attempt was made to model the emissions of exhaust gases such as carbon dioxide, carbon monoxide and nitrogen oxides, but also parameters of PM emissions, including parameters of particle size distribution for number and mass concentration. This research was carried out for specific miniature jet engine and blends of HEFA-SPK fuel with Jet A-1 and developed models are accurate only for this specific engine. Results showed which fuel properties and engine performance parameters impact the most emission parameters and how change of 1 standard deviation of specific input parameter will change the emission of CO, CO_2, NOx and PM. The developed models were validated using 20% randomly selected measurement points which were not used in models development and the validation showed very well fit of the modeled and measured values. In few models, R-squared is small, what may suggest that the relationships between input variables and output variable are non-linear and other kind of regression can fit better, for example polynomial regression. For CO_2, CO and geometric mean diameter for particulate mass distribution, the VIF values were too high to accept that model is without multicollinearity so used coefficients cannot be analyzed as parameters which influence the modeled emission indices, although these models are sufficient to predict emission of CO_2, CO and GMDm. Also R-squared of validation was very high for these parameters. The remaining modeled emission parameters meet all requirements and are suitable for emission prediction and analyze of input parameters which impact the final emission index.

This study bridges a gap in the literature by focusing on modeling the impact of HEFA-SPK blend fuel properties on pollutant emissions in miniature jet engines. Future research should explore a broader range of fuel blends produced through different pathways to expand the applicability of the models to other types of sustainable aviation fuels. Such efforts would support the development of more universal models for this type of miniature engine. Additionally, incorporating data from other engine types powered by various SAFs could enable the creation of a generalized model for emission indices as a function of fuel properties and engine performance. These advancements would contribute to improving the environmental assessment of alternative fuels and support the transition towards greater sustainability in aviation.

REFERENCES

1. Kroyan Y, Wojcieszyk M, Kaario O, Larmi M. Modeling the impact of sustainable aviation fuel properties on end-use performance and emissions in aircraft jet engines. Energy. 2022;255(C). https://doi.org/10.1016/j.energy.2022.124470
2. Detsios N, Theodoraki S, Maragoudaki L, Atsonios K, Grammelis P, Orfanoudakis NG. Recent advances on alternative aviation fuels/pathways: A critical review. Energies. 2023;16:1904. https://doi.org/10.3390/en16041904
3. ASTM International. ASTM D7566: Standard Specification for Aviation Turbine Fuel Containing Synthesized Hydrocarbons. West Conshohocken, PA, USA: ASTM; 2024.
4. Chan TW, Chishty WA, Canteenwalla P, Buote D, Davison CR. Characterization of emissions from the use of alternative aviation fuels. J Eng Gas Turbine Power. 2016;138:011506. https://doi.org/10.1115/GT2015-42122
5. Moore RH, Thornhill KL, Weinzierl B, Sauer D, D'Ascoli E, Kim J, et al. Biofuel blending reduces particle emissions from aircraft engines at cruise conditions. Nature. 2017;543:411–415. https://doi.org/10.1038/nature21420
6. Durdina L, Brem BT, Elser M, Schönenberger D, Siegerist F, Anet JG. Reduction of nonvolatile particulate matter emissions of a commercial turbofan engine at the ground level from the use of a sustainable aviation fuel blend. Environ Sci Technol. 2021;55:14576–14585. https://doi.org/10.1021/acs.est.1c04744

7. Timko MT, Herndon SC, de la Rosa Blanco E, Wood EC, Yu Z, Miake-Lye RC, Corporan E. Combustion products of petroleum jet fuel, a Fischer-Tropsch synthetic fuel, and a biomass fatty acid methyl ester fuel for a gas turbine engine. Combust Sci Technol. 2011;183:1039–1068. https://doi.org/10.1080/00102202.2011.581717
8. Statista Research Department. Green aviation: number of SAF airports worldwide by delivery type 2014–2023. Accessed January 2025. Available from: https://www.statista.com
9. Doliente SS, Narayan A, Tapia JFD, Samsatli NJ, Zhao Y, Samsatli S. Bio-aviation fuel: A comprehensive review and analysis of the supply chain components. Front Energy Res. 2020;8:499009. https://doi.org/10.3389/fenrg.2020.499009
10. Hari TH, Yaakob Z, Binitha NN. Aviation biofuel from renewable resources: Routes, opportunities and challenges. Renew Sustain Energy Rev. 2015;42:1234–1244. https://doi.org/10.1016/j.rser.2014.10.095
11. Kurzawska-Pietrowicz P, Jasiński R. A review of alternative aviation fuels. Energies. 2024;17:3890. https://doi.org/10.3390/en17163890
12. Merkisz J, Pielecha J. The on-road exhaust emissions characteristics of SUV vehicles fitted with diesel engines, Combustion Engines. 2011;50:58–72.
13. Jasiński R, Kurzawska P, Przysowa R. Characterization of particle emissions from a DGEN 380 small turbofan fueled with ATJ blends. Energies. 2021;14:3368. https://doi.org/10.3390/en14123368
14. Jasiński R. Evaluation of nanoparticles mass and size emissions from aircraft engines. PhD thesis. Poznań: Poznan University of Technology; 2019.
15. Siegel AF. Multiple regression. In: Practical business statistics. 6th ed. Amsterdam: Academic Press; 2012;347–416. https://doi.org/10.1016/b978-0-12-385208-3.00012-2
16. Ruan Y. Exploring multiple regression models: key concepts and applications. Sci Technol Eng Chem Environ Prot. 2024;1(7). https://doi.org/10.61173/yjpt3s59
17. Roustaei N. Application and interpretation of linear-regression analysis. Med Health Sci J. 2024;13:151–159. https://doi.org/10.51329/mehdiophthal1506
18. Multiple linear regression. Wiley Series in Probability and Statistics. 2020;1–21. https://doi.org/10.1002/9781119392491.ch1
19. TSI. Engine Exhaust Particle Sizer (EEPS) Spectrometer: Operation and service manual. TSI Inc